


Article

Assessment of Future Land Use/Land Cover Scenarios on the Hydrology of a Coastal Basin in South-Central Chile

Camila Orellana Pereira ¹, Rossana Escanilla-Minchel ², Alejandra Cortés González ³, Hernán Alcayaga ^{4,*}, Mauricio Aguayo ⁵, Miguel Aguayo Arias ⁶ and Alejandro N. Flores ⁷

- ¹ Civil Engineering Department, Universidad Diego Portales, Santiago 8370109, Chile
² School of Geography, University of Leeds, Leeds LS2 9JT, UK
³ Civil Engineering Unit, Department of Water Resources Management, Ministry of Public Works of Chile, Santiago 8370190, Chile
⁴ School of Civil Works, Universidad Diego Portales, Santiago 8370190, Chile
⁵ Faculty of Environmental Sciences, EULA-Chile Centre, University of Concepción, Concepción 4070386, Chile
⁶ Faculty of Natural Resources, Universidad Católica de Temuco, Temuco 4781312, Chile
⁷ Department of Geoscience, Boise State University, Boise, ID 83702, USA
* Correspondence: herman.alcayaga@udp.cl

Abstract: Land use and land cover (LULC) change is one of the clearest representations of the global environmental change phenomenon at various spatial and temporal scales. Chile is worldwide recognized to have areas dedicated to non-native forest plantations that specifically in coastal range show high environmental and economic deterioration, questioning the sustainability of the forestry industry. Currently, there are no studies in Chile that reveal the real effects of the LULC change on the water balance at basin or sub-basin scales associated with future scenarios, which might contribute to territorial decision-making and reveal the real magnitude of the effects of these dynamics. In this study, in order to study LULC dynamics in a coastal basin in South-Central Chile, we assessed and analyzed the effects of future LULC change scenarios on the hydrological processes by generating future synthetic land cover maps from Landsat (Landsat 5 TM and Landsat 8 OLI) image datasets. The hydrological model Soil Water Assessment Tool (SWAT) was calibrated and validated, using hydroclimatic time series, to simulate discharges and other hydrological components over those future LULC scenarios. The LULC future scenarios were projected using combined Markov chain analysis (CA–Markov) and cellular automata algorithms for the near (2025), middle (2035) and far (2045) future. The results revealed that the effects on the different components of the water balance of the basin are not as significant except in the soil water transfer in percolation (increase 72.4%) and groundwater flow (increase 72.5%). This trend was especially observed in sub-basins with non-native forest plantations that dominated land cover in the year 2035, in which an increase of 43.6% in percolation and groundwater flows resulted in increased aquifer recharge and water storage, mainly offset by a decrease of 27% in the evapotranspiration. This work demonstrates the importance of evaluating the impacts of the dynamics of LULC on the hydrological response of a coastal basin, and also on how the land use governance and policy are closely linked to that of water resources.

Keywords: LULC changes; hydrological modeling SWAT; LULC future scenarios; water balance



Citation: Pereira, C.O.; Escanilla-Minchel, R.; González, A.C.; Alcayaga, H.; Aguayo, M.; Arias, M.A.; Flores, A.N. Assessment of Future Land Use/Land Cover Scenarios on the Hydrology of a Coastal Basin in South-Central Chile. *Sustainability* **2022**, *14*, 16363. <https://doi.org/10.3390/su142416363>

Academic Editors: Pawan K Joshi and Rajendra Prasad Shrestha

Received: 15 October 2022

Accepted: 25 November 2022

Published: 7 December 2022

Publisher's Note: MDPI stays neutral with regard to jurisdictional claims in published maps and institutional affiliations.



Copyright: © 2022 by the authors. Licensee MDPI, Basel, Switzerland. This article is an open access article distributed under the terms and conditions of the Creative Commons Attribution (CC BY) license (<https://creativecommons.org/licenses/by/4.0/>).

1. Introduction

Land use and land cover (LULC) change is one of the clearest representations of the global environmental change phenomenon that occurs at various spatial and temporal scales. Such changes have been responsible for the variation in the hydrological response at a watershed scale, modifying the flow regime and accelerating soil erosion [1,2]. LULC changes have become one of the most studied topics in the Earth Sciences community, because human activities are the main cause of LULC changes (e.g., agricultural expansion, logging and infrastructure construction) and the impacts of such changes are directly

related to deforestation and fires [3]. The motivations for these anthropic activities can be summarized as the exploitation of natural resources to fulfill immediate human needs, which results in the degradation of ecosystems [4].

The strong relationship between climate, LULC and hydrology have contributed to the concern for the basic characteristics and planet processes (e.g., soil productivity, biodiversity conservation, aridity and drought, desertification, soil degradation, hydrological processes and climate change [5]). The human use and management of the land cover can modify or disrupt the hydrological processes; for example, changes to the canopy interception, soil infiltration and aquifer recharge, runoff generation, water yields, evapotranspiration rates, flood frequency, concentrations of transported substances (sediments, nutrients and pesticides), snowmelt and accumulation [6].

Globally, several studies have been conducted to assess the impacts of LULC change on hydrology at the watershed scale [7–12], which have had different results depending on the local climate and the territory characteristics (relief, aspect, soil type, geology) in the respective study areas. According to [13], most of the plantations in the world are monocultures composed of species such as Eucalyptus, Pinus, Acacia, Tectona, Picea, Pseudotsuga, Swietenia and Gmelina. Many authors [14–16] have criticized monoculture tree plantations because of negative social and environmental impacts (e.g., loss of productivity and soil fertility, increasing fire risk, alteration of the hydrological cycle and increasing risk of promoting pests), despite their economic benefits.

According to CONAF, the decrease and deterioration of native forests is accelerating in Chile. In fact, during the last two or three decades, between 60,000 to 71,000 hectares of native forest and therefore biodiversity have been lost annually [17]. Among the major causes of the reduction of native forest areas are the substitution by scrublands, non-native forest plantations and agricultural lands, fires, annual degradation by livestock and selective felling [18].

At the regional scale in South-Central Chile, coastal rural areas show high environmental and economic deterioration, headed by a process of natural resource degradation, stemming from productive activities [19]. In addition, problems related to current and future water resources, such as increased frequency in flooding and channel morphology degradation (sediments mining, impoundment, channelization), among others [19,20], have been detected in the aforementioned areas. These environmental effects translate into high costs for the state and a deterioration in the quality and standard of living of the population [21].

Aguayo et al. [2], among others [22–24], have described the changes in LULC in the context of the non-native forest expansion that has affected mainly the South-Central Zone of Chile in recent decades. Other studies have focused on the effects of LULC changes in particular species, such as *Pinus radiata*, on the water balance and the amount of water produced [25–27]. Currently, there are no studies in Chile that have revealed the real effects of the dynamics of LULC on the water balance at basin and sub-basin scales or studies that have considered future scenarios, all of which could contribute to territorial decision-making and reveal the real magnitude of the effects of these dynamics.

Despite significant efforts in this regard, some questions remain unanswered. One of the most critical gaps in the literature is related to the link between LULC changes trends (future scenarios) and the effects on the different hydrological components through different spatial scales (basin and sub-basin scales) in basins with a strong expansion of non-native forest plantations. Considering the latter, the following open questions could be addressed: (i) Is it possible that the effects of LULC changes on the hydrological components can be detected or partially masked when the entire basin is considered? (ii) What could be the future trend in the territory of a basin that has had a dominant land use of accelerated expansion in the past? Moreover, (iii) if the dynamics of LULC changes decelerate, could the effects on the hydrological balance of a basin also be stabilized? The above open questions motivate the main goal of this paper, which is to assess and analyze the effects of LULC changes, considering futures scenarios, on the hydrological processes in a coastal basin

in South-Central Chile. The rest of the paper is organized as follows: Section 2 presents the methodology used (case study information, hydrological model and their calibration and validation, and the model to project the future LULC). Section 3 shows the results, highlighting the change in the different components of the hydrological balance due to future land use. Section 4 presents the discussion of the results. Conclusions are provided at the end.

2. Materials and Methods

This section is composed of four subsections. The first subsection is Section 2.1. Study site, where the basin studied is presented. The second subsection is Section 2.2. Satellite image processing and classification of land uses, where the selection criteria of the images, their treatment and the classification method for the determination of the LULC are indicated. The third subsection is Section 2.3. Hydrological Model, where the performance of the model used to analyze changes in the components of the water balance, including hydroclimatic and land data sources, is described. In the same subsection, the selection process of the calibration parameters of the hydrological model was made is described; as well, the selected values for these parameters and the adjustment indicators for hydrological model are presented. Finally, the Section 2.4. Projection of future land use scenarios subsection provides a description of the computational tools used in the LULC projections, which are used as inputs in the hydrological model to assess the effects of LULC on the components of the water balance.

2.1. Study Site

Chile is one of the first ten countries in the world, and the fifth in the Americas, to have areas dedicated to non-native forest plantations [28]. The El Maule, Ñuble, Biobío and La Araucanía regions represent over 84% (surface equivalent to 2.35 mil. ha) of the current non-native forest plantations in the country, and it is composed mainly of *Pinus radiata* and *Eucalyptus globulus* [29]. This is in part because of the enactment of the Forest Law of 1931, which expresses the state's interest of promoting reforestation for erosion control, and the Law Decree 701 of 1974, which promotes a rapid increase in non-native forest plantations [2], resulting in the reduction of native forest, natural lands and agricultural lands. One of the areas with the largest number of non-native forest plantations in Chile is the Coastal Mountain Range.

The study site corresponds to the Andalién River Basin, located in the Coastal Mountain Range of the Biobío Region, between $36^{\circ}42'$ to $36^{\circ}56'$ S and $72^{\circ}36'$ to $73^{\circ}04'$ W (Figure 1). The basin has a surface of 780 km² and, according to the Köppen classification, the basin has a Mediterranean climate with oceanic influence (Csb) and a pluvial regime [30]. It has an average temperature of 13 °C and four cold months (May–August), where 70% of the annual precipitation is concentrated, ranging between 1200 and 1400 mm [31].

The Csb climate favored the primary occupation of the territory and the intensive use of natural resources, since its native forests have been used from the middle of the 20th century to the present [32]. The Andalién River Basin is one of the most environmentally degraded areas of the region, mainly because of the LULC change [32]. Non-native forest plantations (exotic) and native and mixed forest (which cover 46.0% and 11.8%, respectively) are the main LULC present in the basin as depicted in Figure 1 [31,33]. The Andalién River Basin covers the 23% of the province of Concepción that includes the communes of Penco, Florida, and the city of Concepción [31], with 223,574 inhabitants [33].

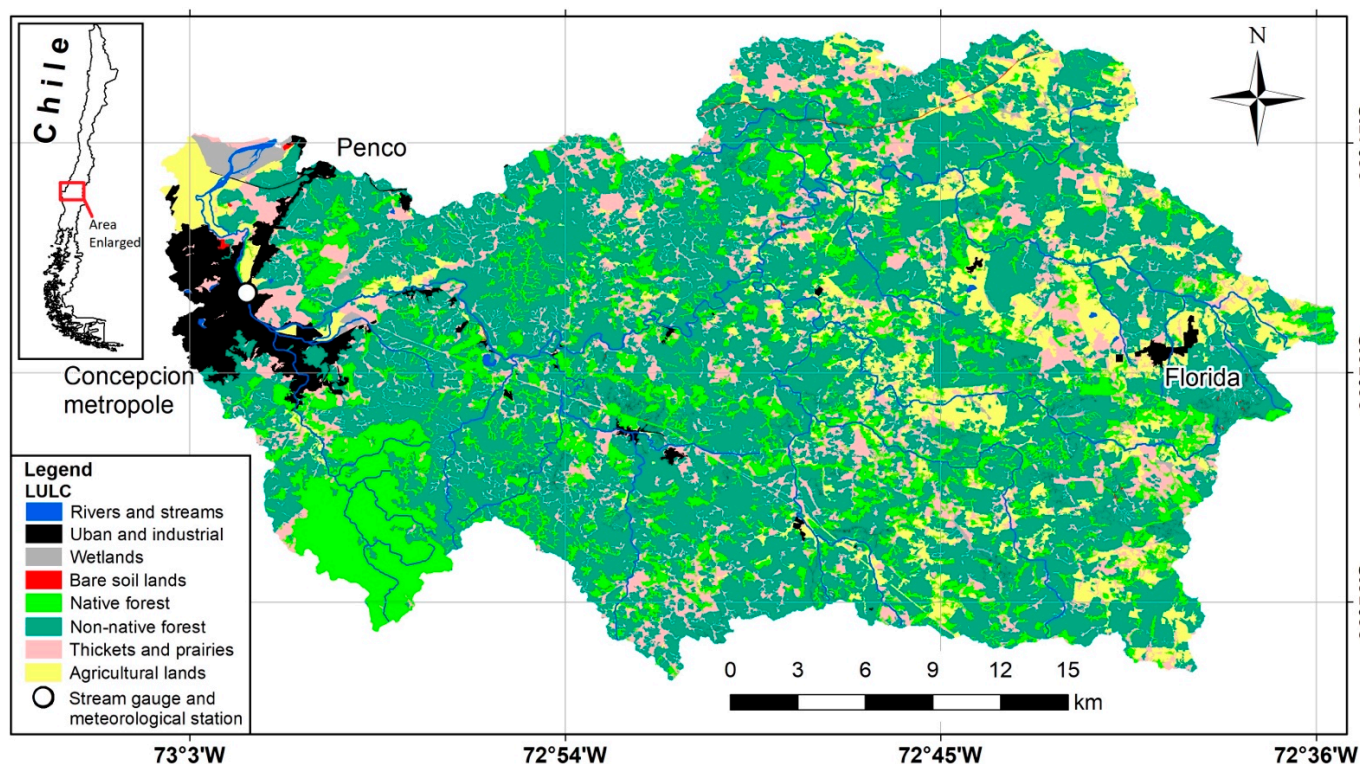


Figure 1. Location of the Andalién River Basin and LULC modified from CONAF [34].

2.2. Satellite Image Processing and Classification of Land Uses

Landsat images of 30 m resolution for the period 2003–2016 were used to analyze the land use dynamics in the basin (Table 1). All images were downloaded from the United States Geological Survey (USGS) database [35]. These classified images were used as input data in the hydrological model, as described in later sections.

Table 1. Satellite images with their acquisition date and resolution, used in the hydrological model.

Satellite Sensor	Acquisition Date
Landsat 5 TM	20 December 2003
	22 February 2004
	24 February 2005
	26 January 2006
	29 January 2007
	16 January 2008
	8 April 2009
	26 March 2010
	29 March 2011
Landsat 8 OLI	9 August 2013
	12 August 2014
	31 August 2015
	18 September 2016

Only Landsat images with less than 10% cloud cover were selected. Next, the atmospheric and radiometric corrections were applied using the advanced FLAASH (Fast Line-of-sight Atmospheric Analysis of Spectral Hypercubes) module available in the ENVI 5.3 software. The advance FLAASH module corrects wavelengths in the visible through near-infrared and shortwave infrared ranges, incorporating the radiation transfer code MODTRAN4 [36]. These corrections to adapt the raw pixel values were made possible

because of the influence generated by the atmosphere during data acquisition and the potential sensor calibration failures caused by radiance [37].

For LULC classification of Landsat images, an interactive supervised classification algorithm was used. The algorithm is available in ArcGIS software version 10.4. [38,39]. This procedure was performed by creating training polygons extracted from two previous LULC classifications made by the National Forestry Corporation (CONAF) for the years 2008 and 2015 [34,40,41]. The training polygons created using the CONAF LULC 2008 were used to classify the set of Landsat images for the period 2003–2011, while the training polygons created using the CONAF LULC 2015 were used to classify the set of Landsat satellite images for the period 2013–2016. The LULC classifications obtained through the Landsat images were complemented by the data provided by the LULC maps developed by Hansen [42]. Determining the accuracy of the classified Landsat images was performed using a confusion matrix to compare the concordance between a set of random sampling points in the classified images with control areas where the surfaces of LULC are known.

The results of LULC classification using the aforementioned methodology were re-grouped into nine categories. As will be explained later, the hydrological modeling was performed using the model Soil and Water Assessment Tool (SWAT) [43]; therefore, these nine LULC were associated with the land use classes in the SWAT database, as shown in Table 2.

Table 2. LULC classes and SWAT codes.

Land Use Classes	Code in SWAT
Native and Mixed Forest	FRST
Adult Plantation (non-native forest)	FRSE
Young Plantation (non-native forest)	RNGB
Agricultural Coverage	AGRL
Urban and Industrial zones	UIDU
Thickets and Prairie	RNGE
Bare soil lands	BARR
Wetlands	WETN
Rivers and Streams	WATR

2.3. Hydrological Model

In this study, the Soil and Water Assessment Tool (SWAT) model was used [43], which has been applied globally to assess the impacts of LULC change [1,44]. Its multiple functions allow us to obtain valued information for each of the components of the water balance.

The SWAT model is a semi-distributed model and discretizes a basin into multiple sub-basins that are—at the same time—discretized into hydrological response units (HRUs). HRUs represent areas grouped using three land variables: (i) soil type, (ii) LULC and (iii) slope class within a sub-basin [5]. In the SWAT model it is assumed that each HRU responds similarly to the weather input (precipitation and temperature). The hydrological cycle simulated by SWAT is based on a hydrological balance that considers the different processes in each HRU.

The meteorological data input corresponds to the minimum and maximum daily temperatures and precipitation. The modeling period considered in this study ranges from 1994 to 2016, with data obtained from the meteorological station called *Río Andalien camino a Penco* (Figure 1). The stream flow data was obtained at the gauge station located at the same place (both stations share the same name) and both stations are controlled by the General Water Directorate (DGA). A digital elevation model (DEM) with 30 m resolution was used, and it was obtained from the Alaska Satellite Facility (ASF) database [45]. This DEM allowed for the basin delineation and river network generation and extraction. The SWAT model also required soil types information, which was obtained from the Natural Resources Information Center [46], and LULC information, which was obtained from the

classification generated from satellite images for the period 2003–2016 (presented in the Section 2.2).

A sensitivity analysis based on a review of previous research performed in similar basins [47–53] was performed in this study in order to identify the more relevant calibration parameters in SWAT. Such calibration parameters have the greatest influence on simulated hydrological processes, particularly on the stream flow results. The values of the parameters were verified using the value ranges according to [54–56].

The modeling simulation period was performed between 1 January 1994 and 31 December 2016, with a warm-up period of nine years from 1994 to 2002, a calibration period of five years from 2003 to 2007 and a validation period of nine years from 2008 to 2016.

The performance of the SWAT model was evaluated through a set of fit indicators, and the model results were compared with observed discharge data from the stream gauge station (Figure 1), comparing observed and simulated stream flow time series.

According to [57], to evaluate the hydrological model performance using quantitative fit indicators, it is necessary to consider at least the coefficient of determination (R^2), the Nash–Sutcliffe efficiency (NSE) and the percentage of bias (PBIAS). Additionally, the Kling–Gupta efficiency (KGE) was incorporated, which corresponds to a decomposition of the NSE function [58]. To classify the performance of the SWAT model applied in the Andalién River Basin, the criterion proposed by Kouchi et al. [59] was used.

2.4. Projection of Future Land Use Scenarios

Future projections of LULC can be modeled through a trend analysis based on past changes and thus estimate the probabilities of changes based on a group of explanatory variables [60]. To project future LULC, the IDRISI Selva GIS software [58] was used. IDRISI Selva combined Markov chain analysis (CA–Markov) and cellular automata algorithms that allow for LULC projections [56,61]. Recent research [62–65] has demonstrated the efficiency of using the CA–Markov model to quantify the effects of LULC change on the hydrological cycle. The CA–Markov model uses a matrix of transition probabilities deduced from the Bayes' equation in order to predict trends in LULC, which is calculated as follows:

$$S_{(t+1)} = P_{ij} \times S_{(t)} \quad (1)$$

where $S_{(t)}$ and $S_{(t+1)}$ are the states of the system at times t and $t + 1$ respectively, and P_{ij} is the transition probability matrix, which is obtained from the following equation [61]:

$$P = \left\| P_{ij} \right\| = \begin{pmatrix} P_{11} & P_{12} & \dots & P_{1n} \\ P_{21} & P_{22} & \dots & P_{2n} \\ \dots & \dots & \dots & \dots \\ P_{n1} & P_{n2} & \dots & P_{nn} \end{pmatrix} \quad (2)$$

With $0 \leq P_{ij} \leq 1$, where P is the Markov transition probability matrix, P_{ij} is the probability of transformation from the current state (i) to another state (j) and P_{mn} is the probability of states at any moment.

These transition models are very useful when the factors that cause changes in the landscape (e.g., socio-economic variables) are difficult to represent analytically (such as mechanical processes) [57]. For the LULC projections in the Andalién River Basin, three LULC classifications were used: these correspond to the years 2008, 2015 and 2020. The first two LULC were classified by CONAF while the LULC for the year 2020 was obtained through the interactive supervised classification algorithm using Landsat imagery as mentioned above. The LULC for 2008 and 2015 were used as reference LULC (defining 2015 as the base year) to predict future LULC maps in decadal increments. The projected years were 2025 (near future), 2035 (middle future) and 2045 (far future). The classification of LULC 2020 (using Landsat) was considered to be the observed LULC 2020 and was compared with the projected LULC 2020 (using the CA–Markov algorithm) to evaluate the performance of the CA–Markov projection model. The CA–Markov model performance in

the LULC projection maps was evaluated using the Kappa statistical indicator, calculated according to Equation (3) [66,67]:

$$Kappa = \frac{P_o - P_c}{1 - P_c} \quad (3)$$

where P_o is the quantity of cells classified correctly and P_c is the hypothetical probability of chance agreement between the observed LULC 2020 map (from Landsat classification) and the projected LULC 2020 map. The Kappa value was classified according to Aliani et al. [65] as can be seen in Table 3:

Table 3. Kappa coefficients and degree of agreement.

Kappa Coefficient	Degree of Agreement
<0.2	Weak
0.21–0.4	Acceptable
0.41–0.6	Moderate
0.61–0.8	Good
0.81–1.0	Very good

Finally, to evaluate the effects of LULC change on the water balance, hydrological simulations were performed with the calibrated SWAT model for the three future LULC scenarios (near 2025, middle 2035 and far 2045). For the three future LULC scenarios, the same meteorological input time series (daily precipitation and maximum and minimum temperature) from the period 1994–2015 was used. Therefore, the results obtained from the components of the hydrological balance were produced exclusively because of the LULC modifications. The components of the hydrological balance considered were evapotranspiration (ET), percolation (PERC), surface runoff (SURQ), lateral subsurface runoff (LAT), groundwater (GW) and water yield (WYLD).

The overall modeling framework (Sections 2.2–2.4) to evaluate the effects of LULC change on the water balance in the Andalién River Basin is based on the three future LULC scenarios is shown in Figure 2.

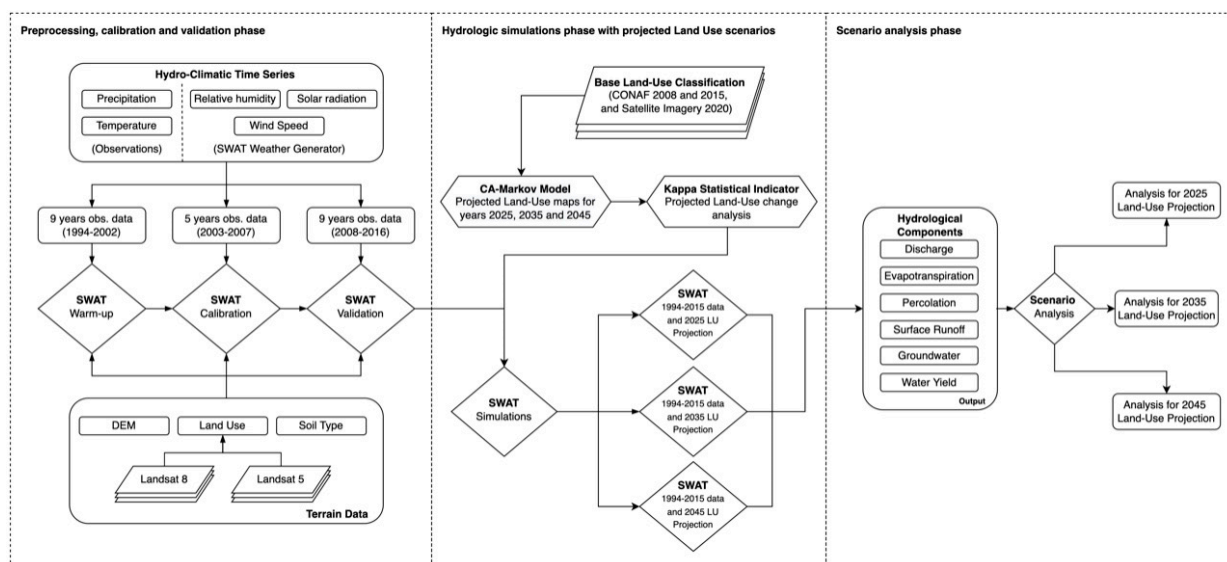


Figure 2. Modeling framework for the evaluation of the effects of LULC changes on the water balance.

3. Results

3.1. Land Use Changes in the Base Years 2008 and 2015

In comparing the LULC between the reference years 2008 and 2015 (Figure 3), the average percentage change was 3.6%. When analyzing the most representative land cover

classes of the basin in terms of surface (FRST, FRSE, RNGB, AGRL and RNGE), we found that the maximum percentage of change was 7.1% for the LULC class of thickets and prairie (RNGE). The LULC that present a greater surface for both reference years are young and adult non-native forest plantations (FRSE and RNGB), native and mixed forest (FRST) and agriculture (AGRL). In 2008, non-native adult forest plantations occupied 46.1% of the surface of the basin, followed by native and mixed forest with 16.5% and finally agriculture with 16.0%. In 2015, a 3.3% decrease in non-native adult forest plantations was observed (possibly due to forest harvesting), which together with non-native young forest plantations corresponded to 56.2% of the basin, showing a clear dominance of non-native forest plantations. On the other hand, agriculture reduced its area by 5.9%, while thickets and prairie increased significantly from 6.8% in 2008 to 13.9% in 2015 (all these data are presented in Supplementary Material S1).

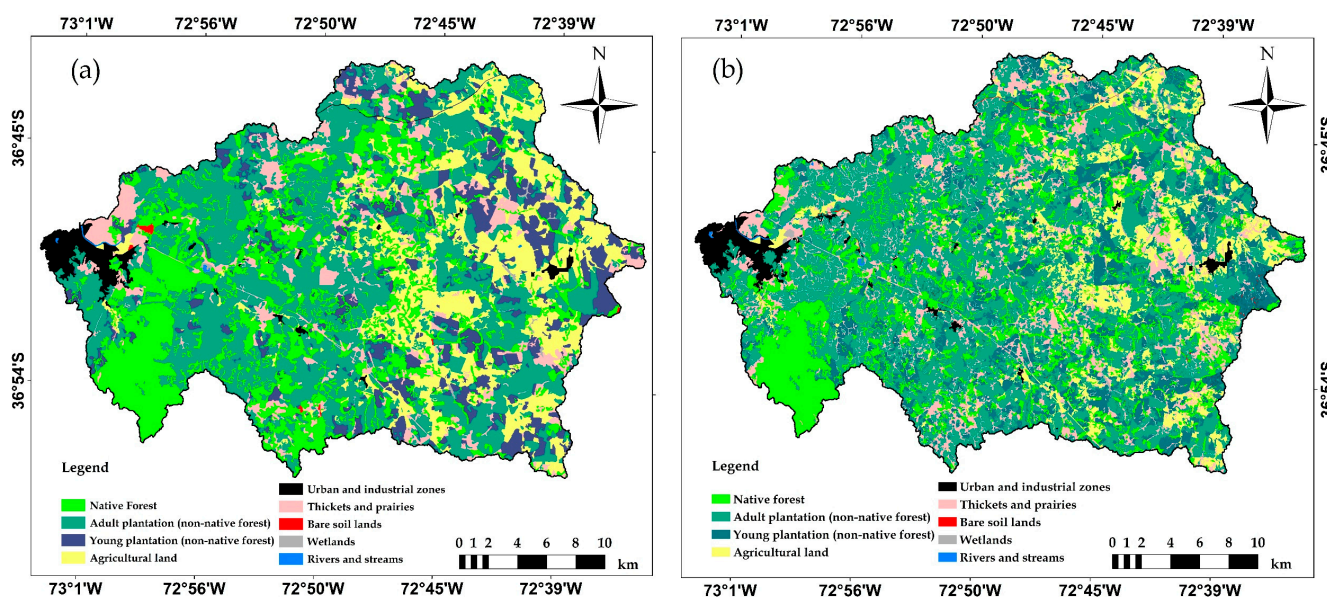


Figure 3. LULC for the reference years 2008 (a) and 2015 (b), from the CONAF LULC classification.

3.2. Warm-Up, Calibration and Validation of the SWAT Hydrological Model

For the three hydrological modeling phases of warm-up, calibration and validation, a time series of 22 years of meteorological data was used, ranging from 1994 to 2016. The first phase was a warm-up of nine years (1994–2002), followed by a five-year calibration period from 2003 to 2007, and finally a nine-year validation period (2008–2016). After completing the sensitivity analysis of the calibration parameters, and based on an extensive review of the literature [47–51], eighteen parameters were selected. These parameters were adjusted using the stream gauge station *Andalien Camino a Penco*. The calibration of the parameters was performed for each of the five years (2003–2007); this information is presented in Supplementary Material S2. Finally, Table 4 shows the results of the hydrological model performance according to the Moriasi criterion [57], using four adjustment indicators for calibration and validation. The results of the hydrological simulations were classified as good (G) and very good (VG). This means that simulated and observed stream flow discharges are numerically close or very close. While the PBIAS values corresponding to -1.18 and -5.67 for calibration and validation show that the model performance is very good and suggest that the stream flows simulated are above the estimated bias.

Figure 4a shows the hyetograph and hydrograph (observed and simulated) for the period 2003–2016, allowing comparison of the results of the model for maximum and minimum stream flow discharge. This figure shows that the model is capable of reproducing base flows better than maximum flows (peak discharges). This fact can be verified in Figure 4b, where there is a greater dispersion for the peak flows.

Table 4. Hydrological model performance.

Adjustment Indicator	Calibration (2003–2007)		Validation (2008–2016)	
R ²	0.91	VG	0.75	G
NSE	0.91	VG	0.73	G
PBIAS	−1.18	VG	−5.67	VG
KGE	0.94	VG	0.85	G

With VG: Very Good; G: Good; S: Satisfactory; U: Unsatisfactory adjustment.

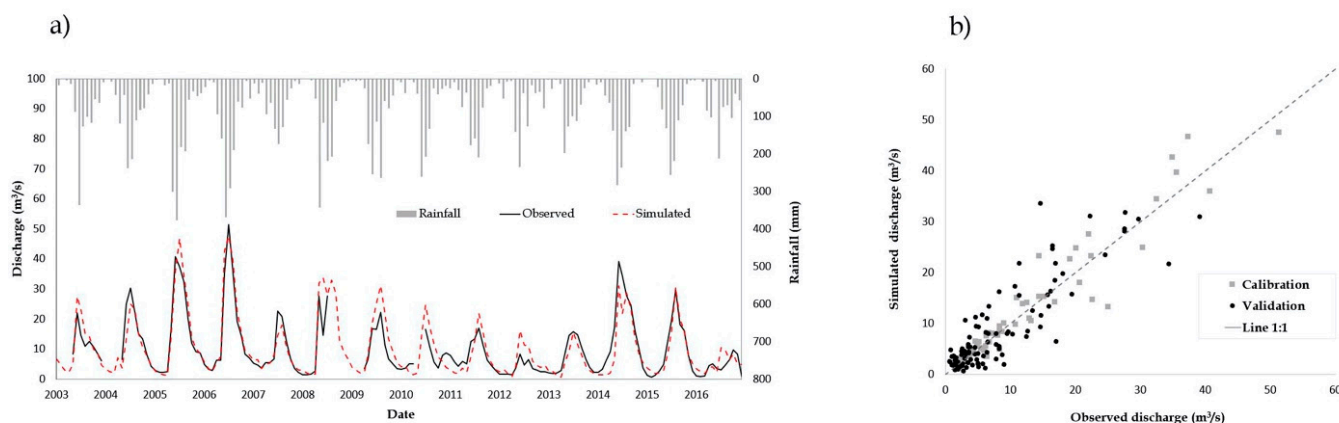


Figure 4. (a) Rainfall and runoff records for both calibration and validation periods and the results of the hydrological model at the Andalien Camino a Penco gauge station and (b) scatter plot for observed and simulated discharge at the Andalien Camino a Penco gauge station.

3.3. Analysis of LULC Projections and Validation

The transition probability matrix, obtained from the LULC reference maps (years 2008 and 2015), is shown in Table 5. The first column with the LULC classes corresponds to the LULC for the year 2015, and the first row represents the expected LULC for the year 2025. The elements of the matrix are the probabilities associated with the expected changes. The red color represents a higher probability of transition and the green color represents a lower probability for the ten-year time frame (2015–2025). The most probable change in coverage corresponds to the transition from native and mixed forest (FRST) to non-native adult forest plantation (FRSE). Additionally, the non-native young forest plantation (RNGB) in 2015 will pass to the status of non-native adult forest plantation in 2025. The probabilities of these transitions occurring are 40.9% and 51.2%, respectively. On the other hand, it was confirmed that there is a 61.7% probability that the industrial and urban zone will remain the same. Finally, there is a 30.4% probability that the bare soil land will become thickets and prairie.

Table 5. Transition probability matrix 2015–2025.

		Probability of Change in 2025:								
LULC Classes		FRST	FRSE	RNGB	AGRL	UIDU	RNGE	BARR	WETN	WATR
LULC in 2015	FRST	0.292	0.409	0.098	0.041	0.002	0.155	0.002	0.002	0.001
	FRSE	0.163	0.428	0.190	0.051	0.006	0.154	0.004	0.003	0.002
	RNGB	0.130	0.512	0.158	0.060	0.002	0.131	0.004	0.004	0.001
	AGRL	0.130	0.293	0.096	0.247	0.007	0.214	0.001	0.012	0.002
	UIDU	0.053	0.133	0.020	0.063	0.617	0.082	0.009	0.002	0.023
	RNGE	0.223	0.365	0.098	0.074	0.015	0.213	0.002	0.009	0.002
	BARR	0.150	0.283	0.081	0.121	0.019	0.304	0.001	0.026	0.014
	WETN	0.123	0.317	0.081	0.140	0.010	0.267	0.002	0.039	0.021
	WATR	0.031	0.204	0.024	0.036	0.336	0.183	0.002	0.008	0.177

The CA–Markov model projected the changes in LULC shown in Table 6. The result of the CA–Markov model shows that for the year 2025 (near future), there will be an increase of 10.6 km² for native and mixed forest (FRST) and 18.6 km² for thickets and prairie (RNGB), corresponding to 1.4% and 2.5% of the basin, respectively. Additionally, the coverage classes non-native adult forest plantation (FRSE) and agricultural (AGRL) will decrease by 16.4 km² and 20.0 km²; this is 2.2% and 2.7% of the basin, respectively.

Table 6. LULC projected for the years 2025, 2035 and 2045.

LULC Classes	2008 (km ²)	2015 (km ²)	Future Scenarios		
			2025 (km ²)	2035 (km ²)	2045 (km ²)
FRST	124.3	126.2	136.8	141.0	142.1
FRSE	346.3	321.4	305.0	305.9	306.0
RNGB	89.7	101.2	107.7	105.4	104.8
AGRL	120.5	75.7	55.7	53.1	52.1
UIDU	16.5	15.9	15.0	15.7	16.4
RNGE	51.4	105.1	123.7	123.3	122.7
BARR	0.9	1.9	2.2	2.1	2.1
WETN	1.7	3.0	3.6	3.5	3.4
WATR	0.6	1.2	1.7	1.8	1.7

In the following periods, these changes will decrease, reaching a stabilization of LULC for a 30-year horizon from the base year 2015. In the period 2025–2035, the average changes are small in comparison with the previous decadal period, presenting an increase of 4.2 km² in FRST and a decrease in agricultural (AGRL) and non-native young forest plantation (RNGB) classes of 2.6 km² and 2.3 km², respectively.

Finally, this stabilization will be consolidated with the following changes for the period 2035–2045: an increase of 1.1 km² in the native and mixed forest (FRST), while for the agriculture (AGRL) and non-native young forest plantation (RNGB) there will be a reduction of 1 km² and 0.6 km², respectively. These changes are negligible and can be considered less than the error associated with the LULC projections by the CA–Markov model.

The spatial distribution of LULC projected in the Andalién River Basin from 2025 to 2045 is shown in Figure 5. From this figure, agriculture (AGRL) appears to be decreasing in the upper part of the basin, being mainly replaced by non-native young forest plantation (RNGB) and thickets and prairie (RNGB).

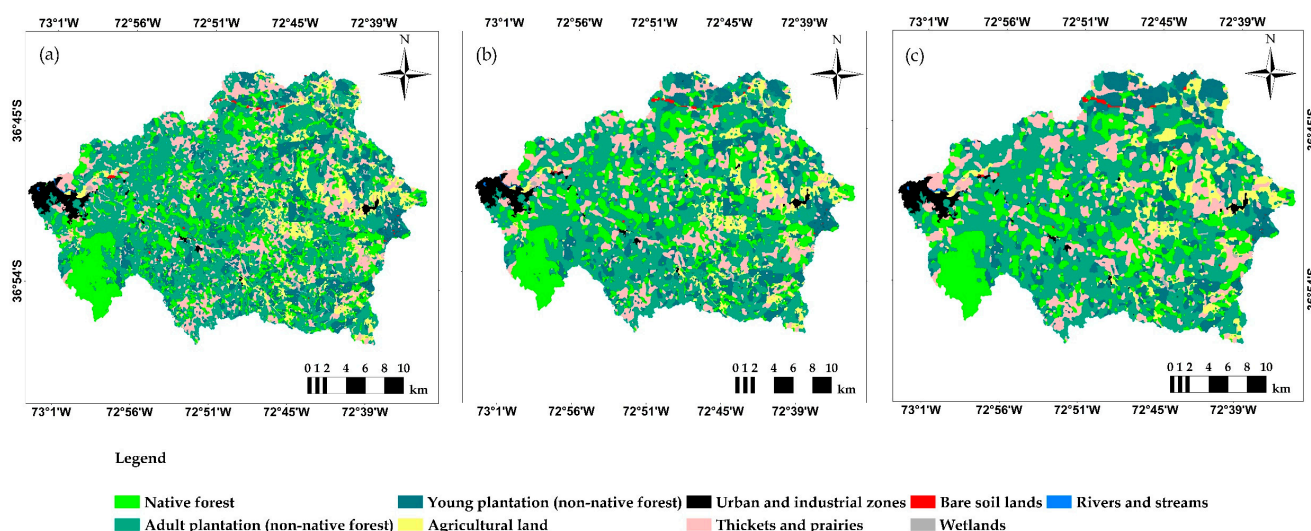


Figure 5. (a) LULC projection maps for 2025; (b) LULC projection map for 2035; (c) LULC projection map for 2045.

The performance of the CA–Markov model was evaluated by comparing the projected LULC for 2020 with the LULC classified (using a Landsat image) for the same year. For this evaluation, the validate tool in the IDRISI Selva software was used, obtaining a Kappa = 0.67. In Figure 6, the surface of each of the observed and projected LULC classes for the year 2020 were compared, with no category having a relative error greater than 10%. Therefore, the LULC projections made using the CA–Markov model have a good precision according to the Landis and Koch criterion [68]. This means that the LULC projections have an accuracy sufficient to be used as input data for the hydrological model. Consequently, the changes in water amounts in the different components of the hydrological balance, due to projected LULC, can be determined.

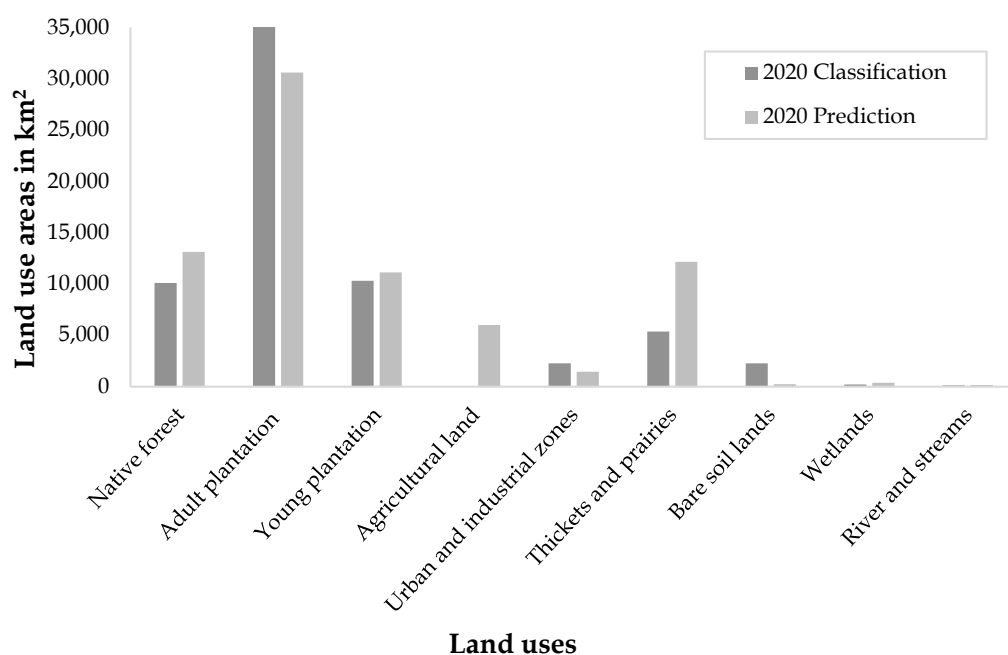


Figure 6. Comparison of LULC observed (Landsat classification) and projected (using CA–Markov), both for the year 2020.

3.4. Hydrological Responses of the Basin and Sub-Basins to the LULC Change Projections

Impacts of land use change on the water balance at basin scale.

The hydrological responses of the Andalién River Basin due to changes in LULC were evaluated using three projected LULC scenarios, considering 2015 to be the base year, and the same climate data series (precipitation and temperature). The hydrological components that were evaluated for each LULC projected scenarios correspond to evapotranspiration (ET), percolation (PERC), surface runoff (SURQ), subsurface runoff (LAT_Q), groundwater (GW_Q), water yield (WYLD) and stream flow discharge of the basin (DISCH).

The results show that on average the annual percolation and groundwater flow increase of 27.4 mm and 12.7 mm, respectively, while the average subsurface runoff decreases in 14.1 mm, under the LULC scenarios projected. In Figure 7, it can be observed that the percolation, groundwater and subsurface runoff components are more susceptible to the LULC future projections, producing maximum variations for 2035, with close to + 80% for groundwater flow and percolation and –20% for subsurface runoff. In contrast, stream flow discharge, evapotranspiration and water yield are the least sensitive. Supplementary Material S4 provides detail of the water balance results for the years 2015, 2025, 2035 and 2045 for each hydrological component.

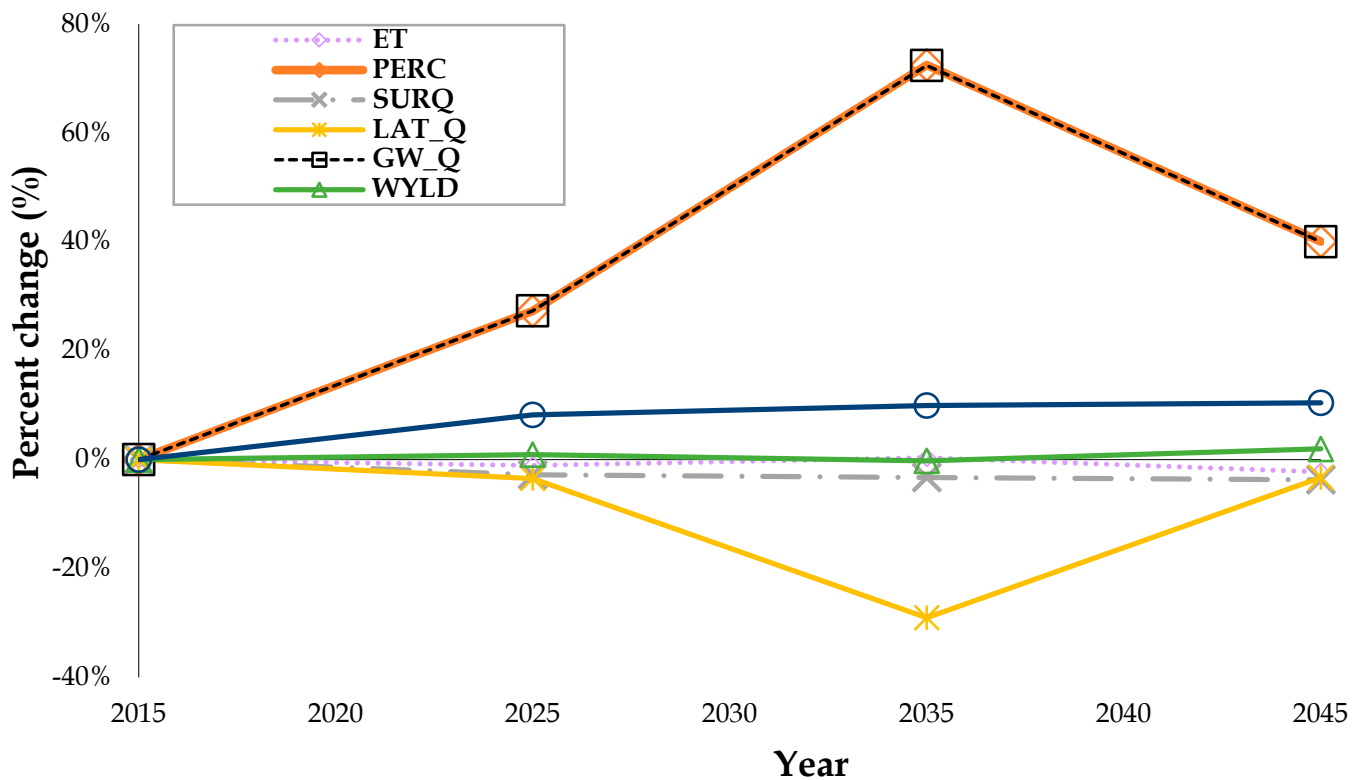
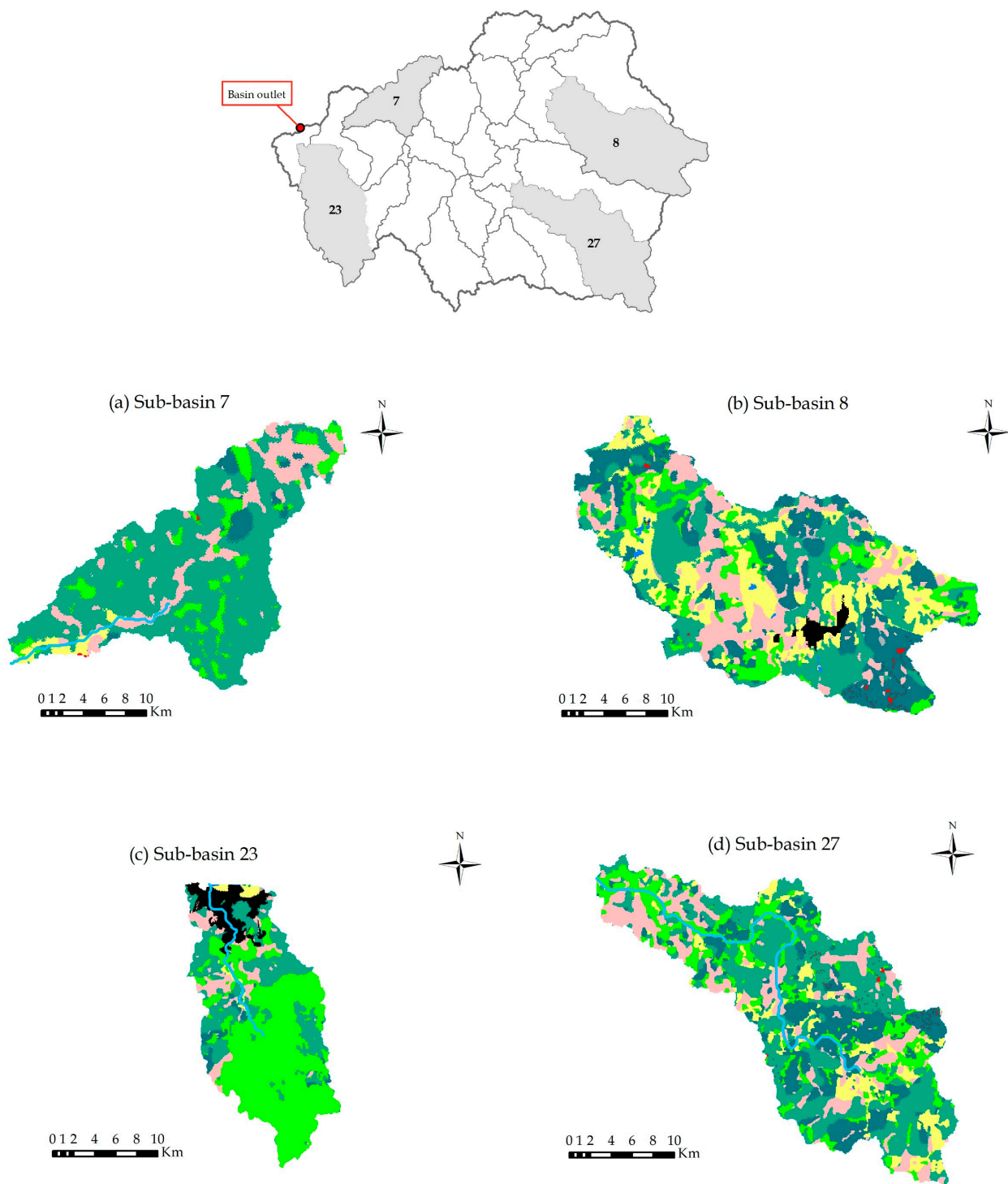


Figure 7. Percentage change of the different components of the hydrological balance for the periods.

Analysis of the water balance in representative LULC sub-basins.

The previous results represent the global balance of the Andalién River Basin, which may mask some local effects in sub-basins where one of the nine LULC classes is dominant. To evaluate this possible mask effect, a detailed analysis was carried out for four sub-basins. These sub-basins were selected based on the largest changes of the dominate LULC of non-native adult and young forest plantation (FRSE and RNGB), agriculture (AGRL), and native and mixed forest (FRST) for the period 2015 to 2045. These sub-basins correspond to those presented in Figure 8, together with their numerical identifier.

In Figure 9, the annual percentage change for each component of the water balance is shown for each of the representative sub-basins. The evapotranspiration graph shows that the greatest increase occurs in sub-basin 27 (the dominant LULC is RNGB) with a 11.7% increase in the year 2045, while a major reduction of 27.3% occurs also in sub-basin 27 (a dominant LULC is RNGB) in the year 2035. Among the largest annual changes, the percolation in sub-basin 27 (the dominant LULC is RNGB) stands out with an increase of 43.6% in 2035. The component that showed significant changes regarding the results of 2015 is groundwater in sub-basin 23 (the dominant LULC is FRST), with an increase of 165%. In addition, Figure 9 shows that the sub-basins 8 (the dominant is AGRL) and 27 (the dominant is RNGB) are the most susceptible to LULC changes projected, which is reflected in the hydrological components, particularly in the projections for the years 2035 and 2045.



Legend

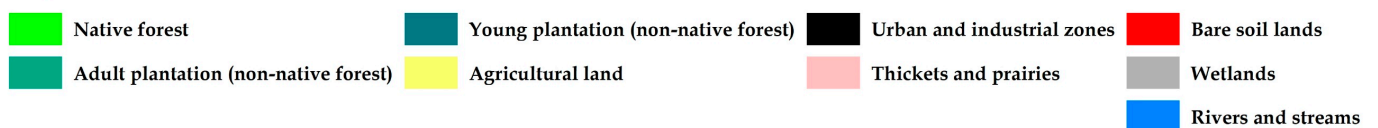


Figure 8. Location of representatives Andalién sub-basins and LULC classes projected for 2025 (a) Sub-basin 7, dominant FRSE; (b) Sub-basin 8, dominant AGRL; (c) Sub-basin 23, dominant FRST; and (d) Sub-basin 27, dominant RNGB.

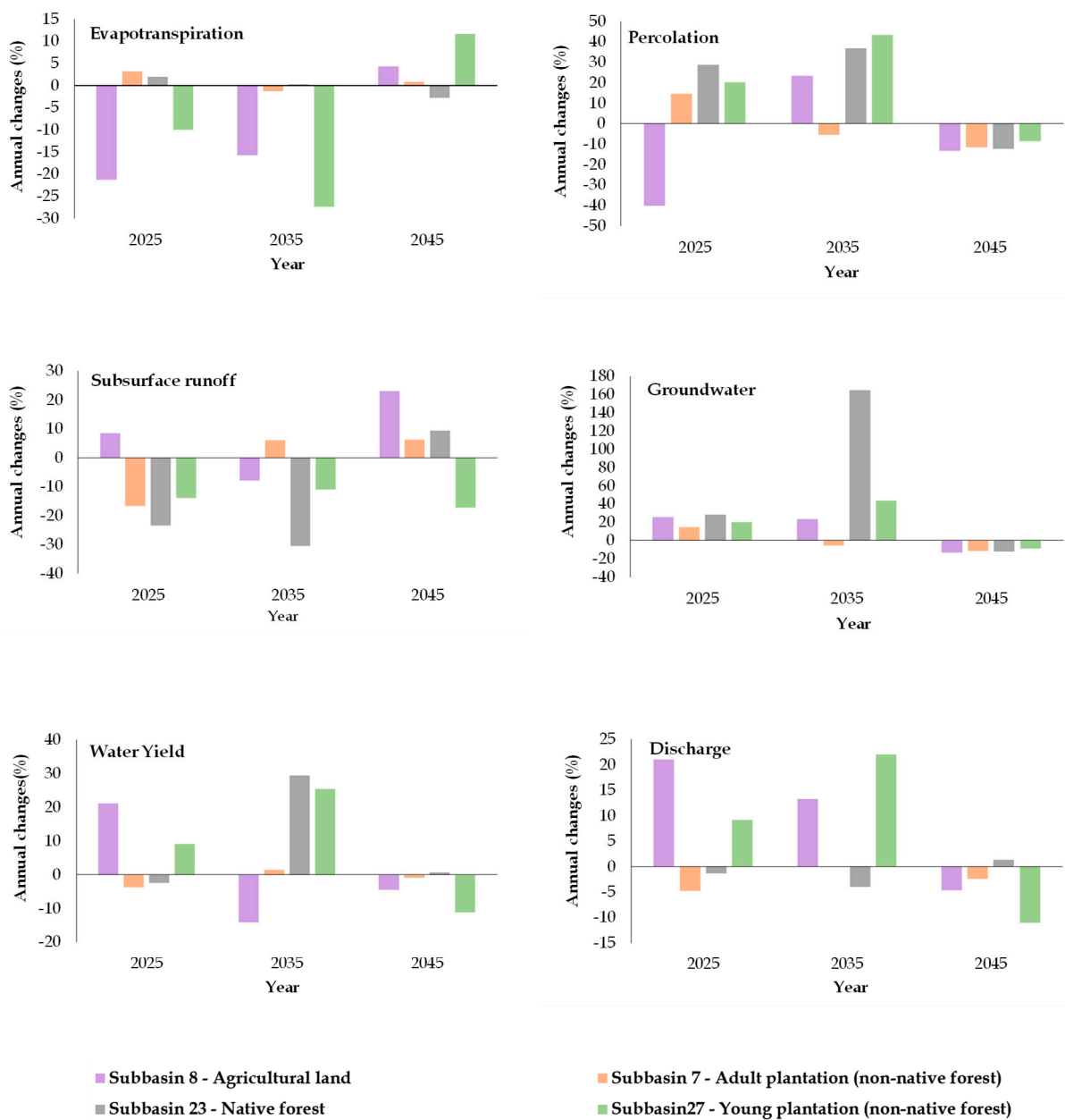


Figure 9. Annual percentage change for hydrological components in representatives LULC sub-basins.

4. Discussion

4.1. Calibration and Validation of the Hydrological Model and Evaluation of the CA–Markov Model

For the calibration phase (2003–2007), the more sensitive parameter was the SCS initial runoff curve number for moisture condition II (CN2). In the validation phase (2008–2016) of the hydrological model, a very good agreement between the observed and simulated monthly mean discharge was determined using statistical indicators R^2 , NSE, PBIAS and KGE [69]. This indicates that the hydrological model is useful for the analysis of hydrological processes in the basin. The model is less efficient in reproducing higher magnitude discharges (Figure 4), overestimating the observed discharges by an average of 3.4%, with the negative PBIAS value confirming this condition. The model is capable in simulating the stream flow discharges, but it was not possible to validate its results for the other hydrological components. Consequently, one of the assumptions of this work is that

the hydrological model can also simulate well the other hydrological processes, as it does with stream flow discharges.

The evaluation of LULC projections, using the CA–Markov model for the year 2020, presented a Kappa coefficient lower than 0.85. This result categorizes the prediction as good [70] in terms of precision. One factor that influences the degree of Kappa agreement is the number of errors induced during the interactive supervised classification process of the Landsat images. Globally, differentiating native forests from non-native forest plantations on as large of a scale as the Andalién River Basin remains a challenge; this complexity makes it difficult in determination of the transformation of native forest to non-native forest plantations, especially for the non-native adult forest plantations [18,71–73].

4.2. Projected Land Use Scenarios

The speed of deforestation globally for the years 2025 and 2050 is likely to be lower compared to the peak period of the 1980s [74]. Currently in Chile, there is scarce information on the projections of the dynamics of LULC in basins like the Andalién River Basin. Some studies in Chile such as Heilmayr et al. [75] mention that despite the rapid expansion of non-native forest plantations at the beginning of the 21st century, a drastic decrease in using native wood in industrial applications, as well as the decrease in the non-native forest conversion rate and changes in forest policies, suggests that plantations relieve demand pressures on native forests. That conclusion is coherent with the results found in this study, since there is a small decreasing trend in non-native forest plantations (young and adult) and a 4.1% increase in the natural LULC (native and mixed forest, thickets and prairie, and wetlands) for the future projections regarding 2015. There are two main forces that can explain the stabilization of non-native forest expansion in the watershed, one of which is the limited expansion space available. Likely there are no more suitable places with the conditions (economic, social and environmental) for non-native forest plantations. The second corresponds to the policy regarding recovery of the native forest and limiting non-native forest development (Law No. 20.283 of 2008), in which the main objective is the protection, recovery and conservation of native forests, to improve forest sustainability [76].

In a comparable study in Africa [77], a similar behavior was reported, where an average LULC change rate of less than 1.0%, with a maximum of 8.5% for one of the LULC classes. Likewise, a study by Nath et al. [70] in China revealed a maximum change rate of 7.9%, while a large number of the classes did not show differences greater than 1% for the projected periods. These reports on the slowdown and subsequent stabilization of non-native forest expansion and deforestation of the native forest are consistent with the projections of LULC change made for the Andalién River Basin for the near (2025), middle (2035) and far (2045) future. For these periods, the land uses remain practically unchanged, breaking the trend of the last three decades (1980, 1990 and 2000) of increased non-native forest expansion.

4.3. Land Use Change Impacts on the Water Balance at Basin and Sub-Basins Scales

The impact on each component of the water balance in the Andalién River Basin was evaluated by maintaining the input climate time series and modifying only the LULC scenarios to reveal the effects of these changes. At the basin scale, the evaluated hydrological components that presented the greatest variability (period 2015–2035) for projected LULC scenarios were percolation (+72.5%), stream flow discharge (+9.9%), subsurface runoff (−29.0%) and groundwater flow (72.4%), which are, according to Tankpa et al. [78], the most important components in a hydrographic basin. According to Yan et al. [7], when a LULC transformation occur from agricultural (AGRL) land cover to thickets and prairie (RNGE), the evapotranspiration increases and consequently surface runoff (SURQ) decreases. This condition is present in the Andalién River Basin, where the probability of transformation is 2.1% (AGRL to RNGE), reducing surface runoff by 3.3% for the average of three projected scenarios.

At the basin scale, the minimal changes (stabilization) of non-native forest expansion can explain the steady state of evapotranspiration (ET) and surface runoff (SURQ). In the basin, the bare soil surface is negligible, a large part of the water transfers through ET and depends directly on plants but above all depends on forests (native and non-native) [24,78,79]. According to the literature [9,80], the amount of ET depends strongly on the ground cover and, consequently, changes in the amount of ET will influence the other components of the water balance. To maximizing the water yield (WYLD) and the discharge (DISCH), a watershed management strategy should focus on reducing the ET.

The results of the hydrological modeling focused on the sub-basins show an important alteration, particularly in the sub-basin that will have a greater coverage of non-native young forest plantations (sub-basin 27). When the non-native young forest plantation becomes the dominant LULC, a reduction in water transfer to the soil (PERC and GW_Q) occurs, with a decrease from LULC 2015 to the LULC 2045 of 318.8 mm to 291.0 mm for PERC, respectively, and a decrease from 148.1 mm to 135.1 mm for GW_Q. In addition, there is a projected increase in ET, from 441.9 mm to 493.5 mm in that same period. The conditions mentioned (an increase in ET and a decrease in PERC and GW) are relevant, because there is a negative effect on the water yield in basins that have extensive, fast-growing, exotic plantations (i.e., pine and eucalyptus), as is the case of sub-basin 27 and the entire Andalién River Basin, where exotic forest plantations (young and adult) cover over 50% of the surface. Researchers [81] indicate that the behavior in the water consumption of the non-native forest plantations produce in the long term a reduction of water in the soil (in terms of moisture and groundwater flows).

5. Conclusions

This study investigated the effects of LULC dynamics on the water balance in the coastal basin of the Andalién River, located in South-Central Chile. Three research questions were raised to improve our understanding of the relationship between land management and its effects on the hydrological cycle in the basin. We have found in this work that the dynamics of LULC practically stopped: after a tremendous expansion of non-native forest plantations in the last three decades in Chile, and particularly in the coastal basins, this expansion has stabilized. LULC projections show that the conditions no longer exist for non-native forest plantations to increase their occupation in the Andalién River Basin. Despite the above, the effects of small changes in LULC can be reflected in the different components of the water balance, with a redistribution of water transfers to each of the components and in different magnitudes, with a non-proportional and non-linear relationship between changes in LULC and effects on the hydrological cycle. When the whole of the Andalién River Basin is considered (780 km² surface), the effects of LULC on the hydrological cycle are reduced since there is compensation due to the different LULC patches that change over time, which makes it difficult to assess how the LULC dynamics affects the hydrological cycle at the outlet of the basin. On the other hand, by focusing the analysis on sub-basins with a specific dominant LULC, as is the case of non-native forest plantations (young and adult), the changes are more evident and their effects can be better quantified, allowing promotion of more effective practices and management in the territory.

The LULC change predictions exhibited a trend towards the stability of the main coverage in the basin and a reduction in native and mixed forest, agricultural land, and non-native forest plantation (young and adult) LULC for the three future scenarios of the years 2025, 2035 and 2045. Despite the dynamics of LULC changes being less than what occurred in the two preceding decades (2000–2020), its consequences on the water balance of the basin, and particularly in the sub-basins, is considerable in terms of the water storage in the soil and the negative effects on water yield. This is especially observed in sub-basins with non-native forest plantations that dominated LULC, in which a decrease in percolation (8.7%) results in reduced aquifer recharge, as well as a decrease in groundwater flows (8.8%), which are mainly offset by an increase in evapotranspiration (11.7%), in the long-term projection (2045). On the other hand, at the basin scale, the semi-distributed

hydrological model made it possible to quantify the hydrological impacts on an annual time scale for the long term (far projection 2045), with an increase in percolation (40.1%) and groundwater flow (40.0%) and a decrease in evapotranspiration (2.2%), surface runoff (3.7%) and subsurface runoff (3.3%). Some measures can be applied to improve water management based on management practices for non-natural of land cover such as non-native forest plantations. The most cultivated forest species in Chile are pine (*pinus radiata*) and eucalyptus (*eucalyptus globulus*), which consume a lot of water [82], increasing the evapotranspiration rates. One of the measures to improve the water management for this type of basin is to replace non-native forest plantations with thickets and prairie, reducing evapotranspiration rates and increasing the surface runoff and water yield [83,84].

In many of the basins in the Chilean territory, there is a dearth of detailed information on agricultural or forest management practices (native and non-native), new industrial projects (private investments), public works (new roads, road improvements, among others), future environmental regulations or economic growth and other variables even more complex such as social behaviors (demographic). This lack of information could represent a limitation for this study. If the information on these variables was available, a hybrid model could be considered within that combines a CA–Markov model and a multi-criteria evaluation (MCE). However, it is probable that the effort put into improving the input data and predictions would not reflect a significant improvement in the assessment of the hydrological balance for a basin the size of the Andalién River Basin.

Finally, the analysis of the LULC change effects is important for decision-making, but a still greater challenge is considering this condition with others that may overlap such as climate change [5,7,44,85].

Supplementary Materials: The following supporting information can be downloaded at: <https://www.mdpi.com/article/10.3390/su142416363/s1>, Figure S1: Percentual comparison of LULC areas for references years 2008 and 2015, based on CONAF; Table S1: Percentual comparison of LULC areas for references years 2008 and 2015, based on CONAF; Table S2: Parameters used in the calibration process; Table S3: Results of the hydrological model performance for the calibration period; Table S4: Results of the hydrological model performance for the validation period; Table S5: Water balance results for the years 2015, 2025, 2035 and 2045.

Author Contributions: Conceptualization, H.A. and M.A.; Methodology, C.O.P.; Validation, H.A., M.A., M.A.A. and A.N.F.; Formal analysis, C.O.P. and M.A.; Investigation, H.A.; Resources, R.E.-M., A.C.G., H.A., M.A., M.A.A. and A.N.F.; Data curation, C.O.P. and A.C.G.; Writing—original draft, C.O.P.; Writing—review & editing, C.O.P., R.E.-M., A.C.G., H.A., M.A. and M.A.A.; Visualization, C.O.P.; Supervision, H.A. and M.A.; Project administration, H.A., M.A. and A.N.F.; Funding acquisition, M.A.A. All authors have read and agreed to the published version of the manuscript.

Funding: This research and the APC was funded by the Interdisciplinary Water Institute Rukako and by the project FEQUIP 2019-INRN-03 both at Universidad Católica de Temuco.

Informed Consent Statement: Not applicable.

Conflicts of Interest: The authors declare no conflict of interest.

References

1. Aghsaei, H.; Mobarghaee Dinan, N.; Moridi, A.; Asadolahi, Z.; Delavar, M.; Fohrer, N.; Wagner, P.D. Effects of dynamic land use/land cover change on water resources and sediment yield in the Anzali wetland catchment, Gilan, Iran. *Sci. Total Environ.* **2020**, *712*, 136449. [[CrossRef](#)] [[PubMed](#)]
2. Aguayo, M.; Pauchard, A.; Azócar, G.; Parra, O. Cambio del uso del suelo en el centro sur de Chile a fines del siglo XX: Entendiendo la dinámica espacial y temporal del paisaje. *Rev. Chil. Hist. Nat.* **2009**, *82*, 361–374. [[CrossRef](#)]
3. Lambin, E.F.; Geist, H.J.; Lepers, E. Dynamics of Land-Use and Land-Cover Change in Tropical Regions. *Annu. Rev. Environ. Resour.* **2003**, *28*, 205–241. [[CrossRef](#)]
4. Foley, J.; Defries, R.; Asner, G.; Barford, C.; Bonan, G.; Carpenter, S.; Chapin III, F.S.; Coe, M.; Daily, G.; Gibbs, H.; et al. Global Consequences of Land Use. *Science* **2005**, *309*, 570–574. [[CrossRef](#)] [[PubMed](#)]
5. Dibaba, W.T.; Demissie, T.A.; Miegel, K. Watershed hydrological response to combined land use/land cover and climate change in highland ethiopia: Finchaa catchment. *Water* **2020**, *12*, 1801. [[CrossRef](#)]

6. Chhabra, A.; Geist, H.; Houghton, R.A.; Haberl, H.; Braimoh, A.K.; Vlek, P.L.G.; Patz, J.; Xu, J.; Ramankutty, N.; Coomes, O.; et al. Multiple Impacts of Land-Use/Cover Change. In *Land-Use and Land-Cover Change*; Springer: Berlin/Heidelberg, Germany; pp. 71–116.
7. Yan, R.; Cai, Y.; Li, C.; Wang, X.; Liu, Q. Hydrological responses to climate and land use changes in a watershed of the Loess Plateau, China. *Sustainability* **2019**, *11*, 1443. [[CrossRef](#)]
8. Li, S.; Yang, H.; Lacayo, M.; Liu, J.; Lei, G. Impacts of land-use and land-cover changes on water yield: A case study in Jing-Jin-Ji, China. *Sustainability* **2018**, *10*, 960. [[CrossRef](#)]
9. Welde, K.; Gebremariam, B. Effect of land use land cover dynamics on hydrological response of watershed: Case study of Tekeze Dam watershed, northern Ethiopia. *Int. Soil Water Conserv. Res.* **2017**, *5*, 1–16. [[CrossRef](#)]
10. Tong, S.T.Y.; Sun, Y.; Ranatunga, T.; He, J.; Yang, Y.J. Predicting plausible impacts of sets of climate and land use change scenarios on water resources. *Appl. Geogr.* **2012**, *32*, 477–489. [[CrossRef](#)]
11. Öztürk, M.; Coptý, N.K.; Saisel, A.K. Modeling the impact of land use change on the hydrology of a rural watershed. *J. Hydrol.* **2013**, *497*, 97–109. [[CrossRef](#)]
12. Petrović, A.M.; Kostadinov, S.; Mustafić, S. The impact of depopulation on reduction of the peaks of torrential floods in selected watersheds of the southeastern Serbia. *Acad. Perspect. Procedia* **2022**, *5*, 201–209. [[CrossRef](#)]
13. Keltý, M.J. The role of species mixtures in plantation forestry. *For. Ecol. Manag.* **2006**, *233*, 195–204. [[CrossRef](#)]
14. Liu, C.L.C.; Kuchma, O.; Krutovsky, K.V. Mixed-species versus monocultures in plantation forestry: Development, benefits, ecosystem services and perspectives for the future. *Glob. Ecol. Conserv.* **2018**, *15*, e00419. [[CrossRef](#)]
15. Freer-Smith, P.; Muys, B.; Bozzano, M.; Drössler, L.; Farrelly, N.; Jactel, H.; Korhonen, J.; Minotta, G.; Nijnik, M.; Orazio, C. *Plantation Forests in Europe: Challenges and Opportunities*; European Forest Institut: Joensuu, Finland, 2019.
16. Erskine, P.D.; Lamb, D.; Bristow, M. Tree species diversity and ecosystem function: Can tropical multi-species plantations generate greater productivity? *For. Ecol. Manag.* **2006**, *233*, 205–210. [[CrossRef](#)]
17. Moraga, J.; Sartori, A. *Estrategia Nacional de Cambio Climático y Recursos Vegetacionales 2017–2025 Chile (ENCCRV CHILE)*; CONAF: Santiago, Chile, 2016; Volume 2.
18. Centro de Análisis de Políticas Públicas Informe País. Estado del Medio Ambiente en Chile. 2018. Available online: <http://www.cr2.cl/wp-content/uploads/2019/12/Informe-pais-estado-del-medio-ambiente-en-chile-2018.pdf> (accessed on 15 May 2022).
19. Castillo, E.J. Geomorfología de la cuenca del río Andalién, Chile. *Rev. Geográfica* **2008**, *143*, 97–116. [[CrossRef](#)]
20. Rojas, O.; Latorre, T.; Pacheco, F.; Araya, M.; Lopez, J.J. Inundaciones fluviales en cuencas costeras mediterráneas de Chile: Recurrencia, factores físicos y efectos hidrogeomorfológicos de su gestión. In *La Zona Costera en Chile: Adaptación y Planificación para la Resiliencia*; Geo-Libros UC: Macul, Santiago, 2019; pp. 79–103. ISBN 978-956-14-2442-5.
21. Rojas, O.; Mardones, M.; Arumí, J.L.; Aguayo, M. Una revisión de inundaciones fluviales en Chile, período 1574-2012: Causas, recurrencia y efectos geográficos. *Rev. Geogr. Norte Gd.* **2014**, *57*, 177–192. [[CrossRef](#)]
22. Rojas, C.; Pino, J.; Basnou, C.; Vivanco, M. Assessing land-use and -cover changes in relation to geographic factors and urban planning in the metropolitan area of Concepción (Chile). Implications for biodiversity conservation. *Appl. Geogr.* **2013**, *39*, 93–103. [[CrossRef](#)]
23. Miranda, A.; Altamirano, A.; Cayuela, L.; Pincheira, F.; Lara, A. Different times, same story: Native forest loss and landscape homogenization in three physiographical areas of south-central of Chile. *Appl. Geogr.* **2015**, *60*, 20–28. [[CrossRef](#)]
24. Martínez-Retureta, R.; Aguayo, M.; Stehr, A.; Sauvage, S.; Echeverría, C.; Sánchez-Pérez, J.-M. Effect of Land Use/Cover Change on the Hydrological Response of a Southern Center Basin of Chile. *Water* **2020**, *12*, 302. [[CrossRef](#)]
25. Huber, A.; Trecaman, R. Efecto de una plantación de *Pinus radiata* en la distribución espacial del contenido de agua del suelo. *Bosque* **2000**, *21*, 37–44. [[CrossRef](#)]
26. Huber, A.; Iroumé, A.; Bathurst, J. Effect of *Pinus radiata* plantations on water balance in Chile. *Hydrol. Process.* **2008**, *22*, 142–148. [[CrossRef](#)]
27. Putuhena, W.M.; Cordery, I. Some hydrological effects of changing forest cover from eucalypts to *Pinus radiata*. *Agric. For. Meteorol.* **2000**, *100*, 59–72. [[CrossRef](#)]
28. Cubbage, F.; Mac Donagh, P.; Sawinski Júnior, J.; Rubilar, R.; Donoso, P.; Ferreira, A.; Hoeflich, V.; Olmos, V.M.; Ferreira, G.; Balmelli, G.; et al. Timber investment returns for selected plantations and native forests in South America and the Southern United States. *New For.* **2007**, *33*, 237–255. [[CrossRef](#)]
29. CONAF. CONAF, por un CHILE Forestal Sustentable. 2013. Available online: http://www.conaf.cl/wp-content/files_mf/1382992046CONAFporunChileForestalSustentable.pdf (accessed on 18 September 2022).
30. IDE Infraestructura de Datos Geoespaciales. Zonas Climáticas de Chile según Koppen-Geiger Escala 1:1.500.000. 2017. Available online: http://www.geoportal.cl/arcgis/rest/services/Otros/chile_uchile_clima_Koppen_Geiger/MapServer (accessed on 18 September 2022).
31. DGA Diagnóstico y Clasificación de los Cursos y Cuerpos de Agua Según Objetivos de Calidad: Cuenca del río Andalién. 2004. Available online: <https://mma.gob.cl/wp-content/uploads/2017/12/Andalien.pdf> (accessed on 15 May 2022).
32. Castillo, E. Diagnóstico de los paisajes mediterráneos costeros. Cuenca del río Andalién, Chile. *Boletín La Asoc. Geógrafos Españoles* **2010**, *54*, 81–97.
33. Instituto Nacional de Estadísticas División Político Administrativa y Censal, Región del BioBío. 2019. Available online: <https://geoarchivos.inec.cl/File/pub/poblacion-y-vivienda-biobio.pdf> (accessed on 15 May 2022).

34. CONAF Catastro y Actualización de los Recursos Vegetacionales y uso de la Tierra (CONAF). 2015. Available online: <https://ide.minagri.gob.cl/geoweb/2019/11/22/planificacion-catastral/> (accessed on 18 September 2022).
35. U.S. Geological Survey Earth Explorer. 2019. Available online: <http://earthexplorer.usgs.gov> (accessed on 18 September 2022).
36. Yuan, J.; Niu, Z. Evaluation of atmospheric correction using FLAASH. In Proceedings of the 2008 International Workshop on Earth Observation and Remote Sensing Applications, Beijing, China, 30 June–2 July 2008; IEEE: Piscataway, NJ, USA, 2008; pp. 1–6.
37. Paz Pellat, F. Correcciones atmosféricas relativas de imágenes de satélite: Patrones invariantes y modelos atmosféricos. *Rev. TERRA Lat.* **2018**, *36*, 1. [[CrossRef](#)]
38. Mamun, A.A.; Mahmood, A.; Rahman, M. Identification and monitoring the change of land use pattern using remote sensing and GIS: A case study of Dhaka City. *IOSR J. Mech. Civ. Eng.* **2013**, *6*, 20–28. [[CrossRef](#)]
39. Lauricella, A.; Cannon, J.; Branting, S.; Hammer, E. Semi-automated detection of looting in Afghanistan using multispectral imagery and principal component analysis. *Antiquity* **2017**, *91*, 1344–1355. [[CrossRef](#)]
40. CONAF. *Catastro de los Recursos Vegetacionales Nativos de Chile Monitoreo de Cambios y Actualizaciones Período 1997–2011*; Corporación Nacional Forestal: Santiago, Chile, 2011.
41. Corporación Nacional Forestal, Ministerio de Agricultura. *Monitoreo de Cambios, Corrección Cartográfica y Actualización del Catastro de los Recursos Vegetacionales Nativos de la Región del Biobío*; Corporación Nacional Forestal: Santiago, Chile, 2018; Available online: <https://biblioteca.digital.gob.cl/handle/123456789/2336> (accessed on 15 May 2022).
42. Hansen, M.C. High-resolution global maps of 21st-century forest cover change. *Science* **2013**, *342*, 850–854. [[CrossRef](#)]
43. Arnold, J.G.; Srinivasan, R.; Muttiah, R.S.; Williams, J.R. Large area hydrologic modeling and assessment part i: Model development. *J. Am. Water Resour. Assoc.* **1998**, *34*, 73–89. [[CrossRef](#)]
44. Wang, S.; Kang, S.; Zhang, L.; Li, F. Modelling hydrological response to different land-use and climate change scenarios in the Zamu River basin of northwest China. *Hydrol. Process.* **2008**, *22*, 2502–2510. [[CrossRef](#)]
45. UAF Alaska Satellite Facility. 2019. Available online: <https://asf.alaska.edu> (accessed on 15 May 2022).
46. CIREN Capas de Información Geográfica Asociadas al Estudio Agrológico de Suelos: Región del Biobío (VIII). 2014. Available online: <https://bibliotecadigital.ciren.cl/handle/20.500.13082/12032> (accessed on 18 September 2022).
47. Stehr, A.; Debels, P.; Romero, F.; Alcayaga, H. Hydrological modelling with SWAT under conditions of limited data availability: Evaluation of results from a Chilean case study. *Hydrol. Sci. J.* **2008**, *53*, 588–601. [[CrossRef](#)]
48. Blanco-Gómez, P.; Jimeno-Sáez, P.; Senent-Aparicio, J.; Pérez-Sánchez, J. Impact of Climate Change on Water Balance Components and Droughts in the Guajoyo River Basin (El Salvador). *Water* **2019**, *11*, 2360. [[CrossRef](#)]
49. Gitau, M.W.; Chaubey, I. Regionalization of SWAT Model Parameters for Use in Ungauged Watersheds. *Water* **2010**, *2*, 849–871. [[CrossRef](#)]
50. Ahmadi, A.; Aghakhani Afshar, A.; Nourani, V.; Pourreza-Bilondi, M.; Besalatpour, A.A. Assessment of MC&MCMC uncertainty analysis frameworks on SWAT model by focusing on future runoff prediction in a mountainous watershed via CMIP5 models. *J. Water Clim. Chang.* **2020**, *11*, 1811–1828. [[CrossRef](#)]
51. Rivas-Tabares, D.; Tarquis, A.M.; Willaarts, B.; De Miguel, Á. An accurate evaluation of water availability in sub-arid Mediterranean watersheds through SWAT: Cega-Eresma-Adaja. *Agric. Water Manag.* **2019**, *212*, 211–225. [[CrossRef](#)]
52. Anjum, M.N.; Ding, Y.; Shangguan, D. Simulation of the projected climate change impacts on the river flow regimes under CMIP5 RCP scenarios in the westerlies dominated belt, northern Pakistan. *Atmos. Res.* **2019**, *227*, 233–248. [[CrossRef](#)]
53. Ruan, H.; Zou, S.; Yang, D.; Wang, Y.; Yin, Z.; Lu, Z.; Li, F.; Xu, B. Runoff Simulation by SWAT Model Using High-Resolution Gridded Precipitation in the Upper Heihe River Basin, Northeastern Tibetan Plateau. *Water* **2017**, *9*, 866. [[CrossRef](#)]
54. Xie, K.; Liu, P.; Zhang, J.; Libera, D.A.; Wang, G.; Li, Z.; Wang, D. Verification of a New Spatial Distribution Function of Soil Water Storage Capacity Using Conceptual and SWAT Models. *J. Hydrol. Eng.* **2020**, *25*, 04020001. [[CrossRef](#)]
55. Aawar, T.; Khare, D. Assessment of climate change impacts on streamflow through hydrological model using SWAT model: A case study of Afghanistan. *Model. Earth Syst. Environ.* **2020**, *6*, 1427–1437. [[CrossRef](#)]
56. van Griensven, A.; Meixner, T.; Grunwald, S.; Bishop, T.; Diluzio, M.; Srinivasan, R. A global sensitivity analysis tool for the parameters of multi-variable catchment models. *J. Hydrol.* **2006**, *324*, 10–23. [[CrossRef](#)]
57. Turner, M.G. Landscape Ecology: The Effect of Pattern on Process. *Annu. Rev. Ecol. Syst.* **1989**, *20*, 171–197. [[CrossRef](#)]
58. Kling, H.; Fuchs, M.; Paulin, M. Runoff conditions in the upper Danube basin under an ensemble of climate change scenarios. *J. Hydrol.* **2012**, *424–425*, 264–277. [[CrossRef](#)]
59. Kouchi, D.H.; Esmaili, K.; Faridhosseini, A.; Sanaeinejad, S.H.; Khalili, D.; Abbaspour, K.C. Sensitivity of Calibrated Parameters and Water Resource Estimates on Different Objective Functions and Optimization Algorithms. *Water* **2017**, *9*, 384. [[CrossRef](#)]
60. Mas, J.-F.; Kolb, M.; Houet, T.; Paegelow, M.; Olmedo, M.C. Una Comparación de Diferentes Enfoques de Modelación de Cambios de Cobertura/uso del Suelo. In Proceedings of the XIV Simposio Internacional SELPER 2010, Guanajuato, México, 8–12 November 2010; Available online: https://halshs.archives-ouvertes.fr/halshs-01063482/file/Mas_etal_una_comparacion_SELPERGto2010.pdf (accessed on 15 May 2022).
61. Kumar, S.; Radhakrishnan, N.; Mathew, S. Land use change modelling using a Markov model and remote sensing. *Geomat. Nat. Hazards Risk* **2014**, *5*, 145–156. [[CrossRef](#)]
62. Nadoushan, M.; Soffianian, A.; Alebrahim, A. Modeling Land Use/Cover Changes by the Combination of Markov Chain and Cellular Automata Markov (CA-Markov) Models. *J. Earth Environ. Health Sci.* **2015**, *1*, 16. [[CrossRef](#)]

63. Hamad, R.; Balzter, H.; Kolo, K. Predicting land use/land cover changes using a CA-Markov model under two different scenarios. *Sustainability* **2018**, *10*, 3421. [CrossRef]
64. Guan, D.J.; Li, H.F.; Inohae, T.; Su, W.; Nagaie, T.; Hokao, K. Modeling urban land use change by the integration of cellular automaton and Markov model. *Ecol. Modell.* **2011**, *222*, 3761–3772. [CrossRef]
65. Aliani, H.; Malmir, M.; Sourodi, M.; Kafaky, S.B. Change detection and prediction of urban land use changes by CA-Markov model (case study: Talesh County). *Environ. Earth Sci.* **2019**, *78*, 1–12. [CrossRef]
66. Scott, W.A. Reliability of Content Analysis: The Case of Nominal Scale Coding. *Public Opin. Q.* **1955**, *19*, 321. [CrossRef]
67. Pan, S.; Liu, D.; Wang, Z.; Zhao, Q.; Zou, H.; Hou, Y.; Liu, P.; Xiong, L. Runoff Responses to Climate and Land Use/Cover Changes under Future Scenarios. *Water* **2017**, *9*, 475. [CrossRef]
68. Landis, J.R.; Koch, G.G. The measurement of observer agreement for categorical data. *Biometrics* **1977**, *33*, 159–174. [CrossRef] [PubMed]
69. Moriasi, D.N.; Arnold, J.G.; Van Liew, M.W.; Bingner, R.L.; Harmel, R.D.; Veith, T.L. Model Evaluation Guidelines for Systematic Quantification of Accuracy in Watershed Simulations. *Trans. ASABE* **2007**, *50*, 885–900. [CrossRef]
70. Nath, B.; Wang, Z.; Ge, Y.; Islam, K.; Singh, R.P.; Niu, Z. Land Use and Land Cover Change Modeling and Future Potential Landscape Risk Assessment Using Markov-CA Model and Analytical Hierarchy Process. *ISPRS Int. J. Geo-Inf.* **2020**, *9*, 134. [CrossRef]
71. Curtis, P.G.; Slay, C.M.; Harris, N.L.; Tyukavina, A.; Hansen, M.C. Classifying drivers of global forest loss. *Science* **2018**, *361*, 1108–1111. [CrossRef] [PubMed]
72. Zhao, Y.; Feng, D.; Yu, L.; Wang, X.; Chen, Y.; Bai, Y.; Hernández, H.J.; Galleguillos, M.; Estades, C.; Biging, G.S.; et al. Detailed dynamic land cover mapping of Chile: Accuracy improvement by integrating multi-temporal data. *Remote Sens. Environ.* **2016**, *183*, 170–185. [CrossRef]
73. Pliscoff, P. Análisis del Estado Actual de los Ecosistemas en dos Cuencas Presentes en Chile Central: Maipo y Maule. 2020. Available online: <http://bibliotecadigital.ciren.cl/handle/20.500.13082/32390> (accessed on 8 September 2022).
74. Pahari, K.; Murai, S. Modelling for prediction of global deforestation based on the growth of human population. *ISPRS J. Photogramm. Remote Sens.* **1999**, *54*, 317–324. [CrossRef]
75. Heilmayr, R.; Echeverría, C.; Fuentes, R.; Lambin, E.F. A plantation-dominated forest transition in Chile. *Appl. Geogr.* **2016**, *75*, 71–82. [CrossRef]
76. Requena Báez, P.V. Ley Sobre Recuperación del Bosque Nativo y Fomento Forestal: Fortalezas y Debilidades del nuevo Cuerpo Legal. 2008; pp. 1–36. Available online: <http://repositorio.unab.cl/xmlui/handle/ria/12891> (accessed on 15 May 2022).
77. Bello, H.O.; Ojo, O.I.; Gbadegehin, A.S. Land Use/land cover change analysis using Markov-Based model for Eleyele Reservoir. *J. Appl. Sci. Environ. Manag.* **2019**, *22*, 1917. [CrossRef]
78. Tankpa, V.; Wang, L.; Awotwi, A.; Singh, L.; Thapa, S.; Atanga, R.A.; Guo, X. Modeling the effects of historical and future land use/land cover change dynamics on the hydrological response of Ashi watershed, northeastern China. *Environ. Dev. Sustain.* **2020**, *23*, 7883–7912. [CrossRef]
79. Aguayo, M.; Stehr, A.; Link, O. Respuesta hidrológica de una cuenca de meso escala frente a futuros escenarios de expansión forestal. *Rev. Geogr. Norte Gd.* **2016**, *65*, 197–214. [CrossRef]
80. Wubie, M.A.; Assen, M.; Nicolau, M.D. Patterns, causes and consequences of land use/cover dynamics in the Gumara watershed of lake Tana basin, Northwestern Ethiopia. *Environ. Syst. Res.* **2016**, *5*, 8. [CrossRef]
81. Oyarzún, C.; Huber, A. Water balance in young plantations of Eucalyptus globulus and Pinus radiata in southern Chile. *Terra* **1999**, *17*, 35–44.
82. Huber, A.; Iroumé, A.; Mohr, C.; Frêne, C. Efecto de plantaciones de Pinus radiata y Eucalyptus globulus sobre el recurso agua en la Cordillera de la Costa de la región del Biobío, Chile. *Bosque* **2010**, *31*, 219–230. [CrossRef]
83. Zhang, L.; Vertessy, R.; Walker, G.; Gilfedder, M.; Hairsine, P. *Afforestation in a Catchment Context: Understanding the Impacts on Water Yield and Salinity*; eWater CRC: Bruce, ACT, Australia, 2007; ISBN 1876810 09 2.
84. Smith, P.J.T. Variation of water yield from catchments under introduced pasture grass and exotic forest, east otago. *J. Hydrol.* **1987**, *26*, 175–184. Available online: <http://www.jstor.org/stable/43944591> (accessed on 10 September 2022).
85. Mekonnen, D.F.; Duan, Z.; Rientjes, T.; Disse, M. Analysis of combined and isolated effects of land-use and land-cover changes and climate change on the upper Blue Nile River basin's streamflow. *Hydrol. Earth Syst. Sci.* **2018**, *22*, 6187–6207. [CrossRef]